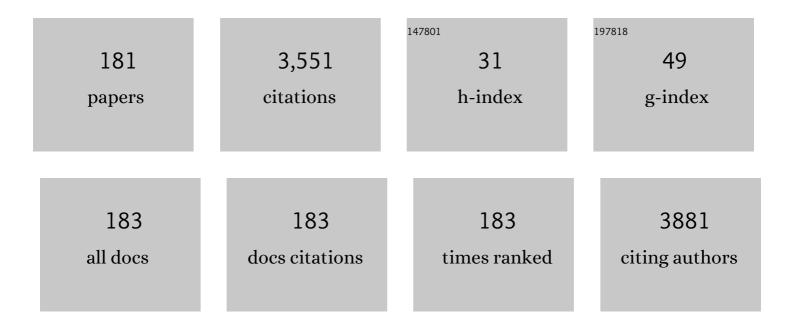
List of Publications by Year in descending order

Source: https://exaly.com/author-pdf/1044903/publications.pdf Version: 2024-02-01



#	Article	IF	CITATIONS
1	Structure and electrical conductivity of nitrogen-doped carbon nanofibers. Carbon, 2009, 47, 1922-1929.	10.3	330
2	Oxidation behavior of multiwall carbon nanotubes with different diameters and morphology. Applied Surface Science, 2012, 258, 6272-6280.	6.1	124
3	Copper on carbon materials: stabilization by nitrogen doping. Journal of Materials Chemistry A, 2017, 5, 10574-10583.	10.3	103
4	Cobalt oxide catalyst for hydrolysis of sodium borohydride and ammonia borane. Applied Catalysis A: General, 2011, 394, 86-92.	4.3	93
5	Raman spectra for characterization of defective CVD multiâ€walled carbon nanotubes. Physica Status Solidi (B): Basic Research, 2014, 251, 2444-2450.	1.5	81
6	In situ XRD study of nanocrystalline cobalt oxide reduction. Kinetics and Catalysis, 2009, 50, 192-198.	1.0	78
7	Effect of Pt addition on sulfur dioxide and water vapor tolerance of Pd-Mn-hexaaluminate catalysts for high-temperature oxidation of methane. Applied Catalysis B: Environmental, 2017, 204, 89-106.	20.2	71
8	Highly dispersed Rh-, Pt-, Ru/Ce0.75Zr0.25O2–δ catalysts prepared by sorption-hydrolytic deposition for diesel fuel reforming to syngas. Applied Catalysis B: Environmental, 2018, 237, 237-244.	20.2	69
9	Development of catalysts for hydrogen generation from hydride compounds. Catalysis Today, 2008, 138, 253-259.	4.4	64
10	Dry reforming of methane over Pt/PrCeZrO catalyst: Kinetic and mechanistic features by transient studies and their modeling. Catalysis Today, 2011, 171, 140-149.	4.4	62
11	Structural features, nonstoichiometry and high-temperature transport in SrFe1â^'xMoxO3â^'δ. Journal of Solid State Chemistry, 2009, 182, 799-806.	2.9	60
12	LiCoO2-based catalysts for generation of hydrogen gas from sodium borohydride solutions. Catalysis Today, 2008, 138, 260-265.	4.4	56
13	Effect of K and Bi doping on the M1 phase in MoVTeNbO catalysts for ethane oxidative conversion to ethylene. Applied Catalysis A: General, 2016, 514, 1-13.	4.3	53
14	Fe/Co/Ni mixed oxide nanoparticles supported on oxidized multi-walled carbon nanotubes as electrocatalysts for the oxygen reduction and the oxygen evolution reactions in alkaline media. Catalysis Today, 2020, 357, 259-268.	4.4	53
15	Multiâ€walled carbon nanotubes with ppm level of impurities. Physica Status Solidi (B): Basic Research, 2010, 247, 2695-2699.	1.5	50
16	Dry reforming of methane over LnFe0.7Ni0.3O3â~'δ perovskites: Influence of Ln nature. Catalysis Today, 2011, 164, 227-233.	4.4	47
17	Magnetic and dielectric properties of carbon nanotubes with embedded cobalt nanoparticles. Carbon, 2017, 114, 39-49.	10.3	45
18	Raman diagnostics of multiâ€wall carbon nanotubes with a small wall number. Physica Status Solidi (B): Basic Research, 2010, 247, 2827-2830.	1.5	40

#	Article	IF	CITATIONS
19	Mechanochemical Synthesis of SiO ₄ ^{4–} â€&ubstituted Hydroxyapatite, Part II – Reaction Mechanism, Structure, and Substitution Limit. European Journal of Inorganic Chemistry, 2014, 2014, 4810-4825.	2.0	40
20	Effect of Bi on catalytic performance and stability of MoVTeNbO catalysts in oxidative dehydrogenation of ethane. Applied Catalysis A: General, 2017, 534, 58-69.	4.3	40
21	Design of functionally graded multilayer thermal barrier coatings for gas turbine application. Surface and Coatings Technology, 2016, 295, 20-28.	4.8	39
22	The effect of support properties on the activity of Pd/C catalysts in the liquid-phase hydrodechlorination of chlorobenzene. Applied Catalysis A: General, 2010, 379, 87-94.	4.3	37
23	Cobalt-boron catalyst for NaBH4 hydrolysis: The state of the active component forming from cobalt chloride in a reaction medium. Molecular Catalysis, 2017, 441, 100-108.	2.0	36
24	Transport features in layered nickelates: correlation between structure, oxygen diffusion, electrical and electrochemical properties. Ionics, 2018, 24, 1181-1193.	2.4	35
25	The investigation of chemical and phase composition of solid precursor of MoVTeNb oxide catalyst and its transformation during the thermal treatment. Applied Catalysis A: General, 2009, 353, 249-257.	4.3	34
26	Structure of Copper Oxide Species Supported on Monoclinic Zirconia. Journal of Physical Chemistry C, 2015, 119, 28828-28835.	3.1	34
27	Platinum nanoparticles supported on nitrogen-containing carbon nanofibers. Catalysis Today, 2012, 186, 42-47.	4.4	33
28	Structure, oxygen transport properties and electrode performance of Ca-substituted Nd2NiO4. Solid State Ionics, 2019, 335, 53-60.	2.7	33
29	Controllable electromagnetic response of onionâ€like carbon based materials. Physica Status Solidi (B): Basic Research, 2008, 245, 2051-2054.	1.5	32
30	Syngas production by CO2 reforming of methane using LnFeNi(Ru)O3 perovskites as precursors of robust catalysts. Catalysis Science and Technology, 2012, 2, 2099.	4.1	32
31	Oxygen transport properties of Ca-doped Pr2NiO4. Solid State Ionics, 2018, 317, 234-243.	2.7	32
32	A modified glycine–nitrate combustion method for one-step synthesis of LaFeO3. Advanced Powder Technology, 2016, 27, 496-503.	4.1	31
33	Functional nanoceramics for intermediate temperature solid oxide fuel cells and oxygen separation membranes. Journal of the European Ceramic Society, 2013, 33, 2241-2250.	5.7	30
34	Structural changes in a nickel–copper catalyst during growth of nitrogen-containing carbon nanofibers by ethylene/ammonia decomposition. Carbon, 2010, 48, 2792-2801.	10.3	29
35	Co metal nanoparticles deposition inside or outside multi-walled carbon nanotubes via facile support pretreatment. Applied Surface Science, 2018, 456, 657-665.	6.1	29
36	Structure of the in situ produced polyethylene based composites modified with multi-walled carbon nanotubes: In situ synchrotron X-ray diffraction and differential scanning calorimetry study. Composites Science and Technology, 2018, 167, 148-154.	7.8	28

#	Article	IF	CITATIONS
37	M5O14-like V–Mo–Nb oxide catalysts: Structure and catalytic performance. Applied Catalysis A: General, 2010, 375, 26-36.	4.3	27
38	Low-temperature synthesis and characterization of apatite-type lanthanum silicatesâ~†. Solid State Ionics, 2008, 179, 1018-1023.	2.7	26
39	Structured nanocomposite catalysts of biofuels transformation into syngas and hydrogen: Design and performance. International Journal of Hydrogen Energy, 2015, 40, 7511-7522.	7.1	26
40	Fe–Mo and Co–Mo Catalysts with Varying Composition for Multiâ€Walled Carbon Nanotube Growth. Physica Status Solidi (B): Basic Research, 2018, 255, 1700260.	1.5	26
41	Electrophysical and Electromagnetic Properties of Pure MWNTs and MWNT/PMMA Composite Materials Depending on Their Structure. Fullerenes Nanotubes and Carbon Nanostructures, 2010, 18, 505-515.	2.1	25
42	Structural and Physical Properties of MWNT/Polyolefine Composites. Fullerenes Nanotubes and Carbon Nanostructures, 2012, 20, 510-518.	2.1	25
43	Mechanochemical Synthesis of SiO ₄ ^{4–} ‣ubstituted Hydroxyapatite, Part I – Kinetics of Interaction between the Components. European Journal of Inorganic Chemistry, 2014, 2014, 4803-4809.	2.0	25
44	The evolution of the M1 local structure during preparation of VMoNbTeO catalysts for ethane oxidative dehydrogenation to ethylene. RSC Advances, 2018, 8, 35903-35916.	3.6	25
45	Transport properties of Ca-doped Ln2NiO4 for intermediate temperature solid oxide fuel cells cathodes and catalytic membranes for hydrogen production. International Journal of Hydrogen Energy, 2020, 45, 13625-13642.	7.1	25
46	Structured catalysts for steam/autothermal reforming of biofuels on heat-conducting substrates: Design and performance. Catalysis Today, 2015, 251, 19-27.	4.4	24
47	Effect of preparation conditions on the phase composition of the MoVTe(Nb) oxide catalyst for the oxidative conversions of propane. Catalysis in Industry, 2010, 2, 291-298.	0.7	23
48	Ni-loaded nanocrystalline ceria-zirconia solid solutions prepared via modified Pechini route as stable to coking catalysts of CH4 dry reforming. Open Chemistry, 2016, 14, 363-376.	1.9	23
49	Photoluminescence of Cr ³⁺ in nanostructured Al ₂ O ₃ synthesized by evaporation using a continuous wave CO ₂ laser. RSC Advances, 2016, 6, 2072-2078.	3.6	23
50	Reinforcement of CVD grown multi-walled carbon nanotubes by high temperature annealing. AIP Advances, 2013, 3, .	1.3	22
51	Preparation of metal-polymer composites through the thermolysis of Fe(II), Co(II), and Ni(II) maleates. Inorganic Materials, 2013, 49, 1055-1060.	0.8	21
52	Comparative study of multiwalled carbon nanotube/polyethylene composites produced via different techniques. Physica Status Solidi (B): Basic Research, 2014, 251, 2437-2443.	1.5	21
53	Co/multi-walled carbon nanotubes as highly efficient catalytic nanoreactor for hydrogen production from formic acid. International Journal of Hydrogen Energy, 2020, 45, 19420-19430.	7.1	21
54	Oxygen mobility and surface reactivity of PrNi1â^xCoxO3+δ–Ce0.9Y0.1O2â^'δ cathode nanocomposites. Solid State Ionics, 2014, 262, 707-712.	2.7	20

#	Article	IF	CITATIONS
55	Peptides on the Surface: Spin-Label EPR and PELDOR Study of Adsorption of the Antimicrobial Peptides Trichogin GA IV and Ampullosporin A on the Silica Nanoparticles. Applied Magnetic Resonance, 2016, 47, 309-320.	1.2	20
56	Effects of the Carbon Support Doping with Nitrogen for the Hydrogen Production from Formic Acid over Ni Catalysts. Energies, 2019, 12, 4111.	3.1	20
57	Alâ€Doped Apatiteâ€Type Nanocrystalline Lanthanum Silicates Prepared by Mechanochemical Synthesis: Phase, Structural and Microstructural Study. European Journal of Inorganic Chemistry, 2008, 2008, 939-947.	2.0	19
58	Effect of complex oxide promoters and Pd on activity and stability of Ni/YSZ (ScSZ) cermets as anode materials for IT SOFC. Catalysis Today, 2008, 131, 226-237.	4.4	19
59	Effect of Pd- precursor and support acid properties on the Pd electronic state and the hydrodesulfurization activity of Pd-zeolite catalysts. Catalysis Today, 2019, 323, 257-270.	4.4	19
60	Luminescence of monoclinic Y2O3:Eu nanophosphor produced via laser vaporization. Optical Materials, 2020, 104, 109843.	3.6	19
61	Raman Spectra for Characterization of Onion-Like Carbon. Journal of Nanoelectronics and Optoelectronics, 2013, 8, 106-109.	0.5	19
62	Activity of Rh/TiO2 catalysts in NaBH4 hydrolysis: The effect of the interaction between RhCl3 and the anatase surface during heat treatment. Kinetics and Catalysis, 2008, 49, 568-573.	1.0	18
63	Optical limiting and bleaching effects in a suspension of onion-like carbon. Quantum Electronics, 2009, 39, 342-346.	1.0	18
64	Formation of active component of MoVTeNb oxide catalyst for selective oxidation and ammoxidation of propane and ethane. Studies in Surface Science and Catalysis, 2010, , 479-482.	1.5	18
65	Solid oxide fuel cell composite cathodes based on perovskite and fluorite structures. Journal of Power Sources, 2011, 196, 7104-7109.	7.8	18
66	Oxygen mobility and surface reactivity of PrNi1â^'xCoxO3â^'δperovskites and their nanocomposites with Ce0.9Y0.1O2â^δby temperature-programmed isotope exchange experiments. Solid State Ionics, 2015, 273, 35-40.	2.7	18
67	Influence of surface layer conditions of multiwall carbon nanotubes on their electrophysical properties. Diamond and Related Materials, 2010, 19, 964-967.	3.9	17
68	Synthesis of Nanoscale <mml:math xmlns:mml="http://www.w3.org/1998/Math/MathML"><mml:mrow><mml:msub><mml:mrow><mml:mtext>TiC Study of the Effect of Their Crystal Structure on Single Cell Response. Scientific World Journal, The, 2012, 2012, 1-14.</mml:mtext></mml:mrow></mml:msub></mml:mrow></mml:math) <td>ext_{}<}/mml:m</td>	ext _{}<} /mml:m
69	Structure Formation of Zinc-Substituted Hydroxyapatite during Mechanochemical Synthesis. Inorganic Materials, 2020, 56, 402-408.	0.8	17
70	The structure and catalytic properties of amorphous phase in MoVTeO catalysts for propane ammoxidation. Applied Catalysis A: General, 2014, 476, 91-102.	4.3	16
71	Structural and transport properties of doped LAMOX — Electrolytes for IT SOFC. Solid State Ionics, 2016, 288, 103-109.	2.7	16
72	The Nature of Synergetic Effect of Manganese Oxide and Platinum in Pt–MnOX–Alumina Oxidation Catalysts. Topics in Catalysis, 2017, 60, 52-72.	2.8	16

#	Article	IF	CITATIONS
73	Fast hydrogen generation from solid NH3BH3 under moderate heating and supplying a limited quantity of CoCl2 or NiCl2 solution. Renewable Energy, 2018, 121, 722-729.	8.9	16
74	Novel proton-conducting nanocomposites for hydrogen separation membranes. Solid State Ionics, 2018, 322, 69-78.	2.7	16
75	Mono-, Bi-, and Trimetallic Catalysts for the Synthesis of Multiwalled Carbon Nanotubes Based on Iron Subgroup Metals. Journal of Structural Chemistry, 2020, 61, 640-651.	1.0	16
76	Structural and electromagnetic properties of Fe2Co-multi-walled carbon nanotubes-polystyrene based composite. Journal of Alloys and Compounds, 2020, 844, 156107.	5.5	16
77	Spinel-type MnxCr3-xO4-based catalysts for ethanol steam reforming. Applied Catalysis B: Environmental, 2021, 283, 119656.	20.2	16
78	Design and characterization of LSM/ScCeSZ nanocomposite as mixed ionic–electronic conducting material for functionally graded cathodes of solid oxide fuel cells. Solid State Ionics, 2011, 192, 540-546.	2.7	15
79	A solid glycine-based precursor for the preparation of La2CuO4 by combustion method. Ceramics International, 2015, 41, 1869-1878.	4.8	15
80	Kinetic Regularities of Methane Dry Reforming Reaction on Nickel-Containing Modified Ceria–Zirconia. Energies, 2021, 14, 2973.	3.1	15
81	Synthesis and properties of nanocomposites with mixed ionic-electronic conductivity on the basis of oxide phases with perovskite and fluorite structures. Glass Physics and Chemistry, 2007, 33, 320-334.	0.7	14
82	Interrelation between catalytic activity for oxygen electroreduction and structure of supported platinum. Journal of Electroanalytical Chemistry, 2014, 729, 34-42.	3.8	14
83	Size-dependent photoluminescence of europium in alumina nanoparticles synthesized by cw CO2 laser vaporization. Journal of Alloys and Compounds, 2020, 815, 152476.	5.5	14
84	New Multicomponent MoVSbNbCeO _x /SiO ₂ Catalyst with Enhanced Catalytic Activity for Oxidative Dehydrogenation of Ethane to Ethylene. ChemCatChem, 2020, 12, 4149-4159.	3.7	14
85	Synthesis, structure and optical properties of the laser synthesized Al2O3 nanopowders depending on the crystallite size and vaporization atmosphere. Advanced Powder Technology, 2021, 32, 2733-2742.	4.1	14
86	Mechanochemical Synthesis of Fe-Doped Apatite-Type Lanthanum Silicates. European Journal of Inorganic Chemistry, 2010, 2010, 589-601.	2.0	13
87	The effect of microwave sintering on stability and oxygen mobility of praseodymium nickelates-cobaltites and their nanocomposites. Solid State Ionics, 2016, 288, 76-81.	2.7	13
88	Methane dry reforming over Ni catalysts supported on Ce–Zr oxides prepared by a route involving supercritical fluids. Open Chemistry, 2017, 15, 412-425.	1.9	13
89	Novel Ni/Ce(Ti)ZrO2 Catalysts for Methane Dry Reforming Prepared in Supercritical Alcohol Media. Energies, 2020, 13, 3365.	3.1	13
90	Structured catalysts with mesoporous nanocomposite active components for transformation of biogas/biofuels into syngas. Catalysis Today, 2021, 379, 166-180.	4.4	13

#	Article	IF	CITATIONS
91	Nitrogen and Oxygen Functionalization of Multiâ€Walled Carbon Nanotubes for Tuning the Bifunctional Oxygen Reduction/Oxygen Evolution Performance of Supported FeCo Oxide Nanoparticles. ChemElectroChem, 2021, 8, 2803-2816.	3.4	13
92	Synthesis, structure and photoluminescent properties of Eu:Gd2O3 nanophosphor synthesized by cw CO2 laser vaporization. Journal of Luminescence, 2021, 235, 118050.	3.1	13
93	Investigation of Fe-Co catalyst active component during multi-walled carbon nanotube synthesis by means of synchrotron radiation X-ray diffraction. Bulletin of the Russian Academy of Sciences: Physics, 2013, 77, 155-158.	0.6	12
94	Maleates of Mn(II), Fe(II), Co(II), and Ni(II) as precursors for synthesis of metal-polymer composites. Russian Journal of Inorganic Chemistry, 2014, 59, 1180-1186.	1.3	12
95	A novel approach to the synthesis of silicocarnotite. Materials Letters, 2016, 164, 255-259.	2.6	12
96	Laser vaporized CrOx/Al2O3 nanopowders as a catalyst for isobutane dehydrogenation. Materials Characterization, 2020, 169, 110664.	4.4	12
97	La2Zr2O7/LaAlO3 composite prepared by mixing precipitated precursors: Evolution of its structure under sintering. Materials Chemistry and Physics, 2020, 251, 123093.	4.0	12
98	Thermolysis of copper(II) salts of maleic acid. Synthesis of metal-polymer composites. Russian Journal of Coordination Chemistry/Koordinatsionnaya Khimiya, 2013, 39, 415-420.	1.0	11
99	Mechanochemical Synthesis of Hydroxyapatite and Its Modifications: Composition, Structure, and Properties. Russian Physics Journal, 2014, 56, 1176-1182.	0.4	11
100	The structure and texture genesis of apatite-type lanthanum silicates during their synthesis by co-precipitation. Ceramics International, 2015, 41, 13393-13408.	4.8	11
101	The Effect of Heat-Treatment Temperature of Cobalt–Boron Catalysts on Their Activity in Sodium Borohydride Hydrolysis. Topics in Catalysis, 2016, 59, 1431-1437.	2.8	11
102	Superparamagnetic behaviour of metallic Co nanoparticles according to variable temperature magnetic resonance. Physical Chemistry Chemical Physics, 2021, 23, 2723-2730.	2.8	10
103	La0.8Sr0.2Ni0.4Fe0.6O3–Ce0.8Gd0.2O2–δNanocomposite as Mixed Ionic–Electronic Conducting Material for SOFC Cathode and Oxygen Permeable Membranes: Synthesis and Properties. Composite Interfaces, 2009, 16, 407-431.	2.3	9
104	Structure and Electrophysical Properties of Multiwalled Carbon Nanotube/Polymethylmethacrylate Composites Prepared via Coagulation Technique. Nanoscience and Nanotechnology Letters, 2011, 3, 18-23.	0.4	9
105	Oxidative dehydrogenation of ethane over M1 MoVNbTeO catalysts modified by the addition of Nd, Mn, Ga or Ge. Catalysis Today, 2021, 361, 50-56.	4.4	9
106	Design and Characterization of Nanocomposites Based on Complex Perovskites and Doped Ceria as Advanced Materials for Solid Oxide Fuel Cell Cathodes and Membranes. Materials Research Society Symposia Proceedings, 2008, 1098, 1.	0.1	8
107	Design and Characterization of Functionally Graded Cathode Materials for Solid Oxide Fuel Cells. ECS Transactions, 2009, 25, 2403-2412.	0.5	8
108	Studies of oxygen transport mechanism in electrolytes based on doped lanthanum silicate with apatite structure using techniques of oxygen isotopic heteroexchange and impedance spectroscopy. Russian Journal of Electrochemistry, 2011, 47, 427-441.	0.9	8

#	Article	IF	CITATIONS
109	Structural Features and Transport Properties of La(Sr)Fe _{1-x} Ni _x O _{3-δ} – Ce _{0.9} Gd _{0.1} O _{2-δ} Nanocomposites—Advanced Materials for IT SOFC Cathodes. Heat Transfer Engineering, 2013, 34, 904-916.	1.9	8
110	Ethanol selective oxidation into syngas over Pt-promoted fluorite-like oxide: SSITKA and pulse microcalorimetry study. Catalysis Today, 2016, 278, 157-163.	4.4	8
111	Effect of Glycine Addition on Physicochemical and Catalytic Properties of Mn, Mn–La and Mn–Ce Monolithic Catalysts Prepared by Solution Combustion Synthesis. Catalysis Letters, 2019, 149, 2535-2551.	2.6	8
112	CO2 Methanation: Nickel–Alumina Catalyst Prepared by Solid-State Combustion. Materials, 2021, 14, 6789.	2.9	8
113	Low-Temperature Synthesis Methods of Doped Apatite-Type Lanthanum Silicates. Journal of Chemical Engineering of Japan, 2007, 40, 1187-1191.	0.6	7
114	Regularities of thermolysis for the Fe(II), Co(II), and Ni(II) salts of maleic and ortho-phthalic acids with the formation of metal/polymer composites. Russian Journal of Coordination Chemistry/Koordinatsionnaya Khimiya, 2017, 43, 446-452.	1.0	7
115	Amorphous ferromagnetic cobalt-boron composition reduced by sodium borohydride: Phase transformation at heat-treatment and its influence on the catalytic properties. Colloids and Surfaces A: Physicochemical and Engineering Aspects, 2018, 537, 485-494.	4.7	7
116	Thermal Decomposition in Systems of Acid Zn(II), Co(II), and Ni(II) Maleates with the Formation of Metallic Nanoparticles. Russian Journal of Physical Chemistry A, 2018, 92, 2247-2252.	0.6	7
117	Multicomponent MoVSbNbGdOx/SiO2 catalyst in oxidative dehydrogenation of ethane: Effect of Gd on catalytic properties. Applied Catalysis A: General, 2022, 633, 118536.	4.3	7
118	Intermediate Temperature Solid Oxide Fuel Cells Based on Nano-Composite Cathode Structures. ECS Transactions, 2008, 13, 275-284.	0.5	6
119	Effect of thermal treatment conditions on the phase composition and structural characteristics of V-Mo-Nb-O catalysts. Kinetics and Catalysis, 2009, 50, 48-56.	1.0	6
120	Photoinduced transparency of a suspension of onion-like carbon nanoparticles. Technical Physics Letters, 2009, 35, 162-165.	0.7	6
121	TEMPERATURE DEPENDENCIES OF CONDUCTIVITY OF MULTI-WALLED CARBON NANOTUBES AND ONION-LIKE CARBON IN DIFFERENT GASEOUS MEDIUM. International Journal of Nanoscience, 2009, 08, 19-22.	0.7	6
122	The Formation of Perovskite during the Combustion of an Energy-Rich Glycine–Nitrate Precursor. Materials, 2020, 13, 5091.	2.9	6
123	Structural, Textural, and Catalytic Properties of Ni-CexZr1â^'xO2 Catalysts for Methane Dry Reforming Prepared by Continuous Synthesis in Supercritical Isopropanol. Energies, 2020, 13, 3728.	3.1	6
124	Nanostructured PtZn intermetallic compound: Controlled formation from PtZn(CH3COO)4 molecular precursor and tests of catalytic properties. Intermetallics, 2021, 132, 107160.	3.9	6
125	CO _x â€free catalytic decomposition of methane over solution combustion synthesis derived catalyst: Synthesis of hydrogen and carbon nanofibers. International Journal of Energy Research, 2022, 46, 11957-11971.	4.5	6
126	Dielectric properties of MWCNT based polymer composites close and below percolation threshold. Physica Status Solidi C: Current Topics in Solid State Physics, 2009, 6, 2814-2816.	0.8	5

#	Article	IF	CITATIONS
127	Mechanochemical Synthesis of SiO ₄ ^{4–} ‣ubstituted Hydroxyapatite, Part III – Thermal Stability. European Journal of Inorganic Chemistry, 2016, 2016, 1866-1874.	2.0	5
128	Thermolysis characteristics of salts of o-phthalic acid with the formation of Fe, Co, Ni, Cu metal particles. Russian Journal of Physical Chemistry A, 2016, 90, 1206-1211.	0.6	5
129	Structure and properties of Pd–Mn hexaaluminate catalysts modified with platinum for the high-temperature oxidation of methane. Kinetics and Catalysis, 2016, 57, 528-539.	1.0	5
130	Combustion characteristics and structure of carbon nanotube/titanium composites. Journal of Thermal Analysis and Calorimetry, 2019, 137, 1903-1910.	3.6	5
131	Chemical Vapor Deposition of Silicon Nanoparticles on the Surface of Multiwalled Carbon Nanotubes. Journal of Structural Chemistry, 2020, 61, 617-627.	1.0	5
132	Carbon Dioxide Conversion of Methane into Synthesis-Gas on Glass Cloth Catalysts. Eurasian Chemico-Technological Journal, 2015, 12, 97.	0.6	5
133	Effect of the lead speciation on a natural freshwater ecosystem. Mendeleev Communications, 2000, 10, 164-165.	1.6	4
134	Nanocrystalline Doped Ceria-Zirconia Fluorite-Like Solid Solutions Promoted by Pt: Structure, Surface Properties and Catalytic Performance in Syngas Generation. Materials Research Society Symposia Proceedings, 2006, 988, 1.	0.1	4
135	Direct synthesis of nitrogen-containing filamentous carbon on a high-percentage Ni-Cu catalyst. Kinetics and Catalysis, 2007, 48, 103-115.	1.0	4
136	Unusual bulk amorphization of gibbsite into atomic size aluminum-oxygen complexes occurring within initial microcrystals under microwave radiation. Doklady Physical Chemistry, 2012, 445, 128-133.	0.9	4
137	A tem study of MoVTe(Nb) oxide catalysts for the selective conversion of propane. Journal of Structural Chemistry, 2014, 55, 962-971.	1.0	4
138	Synthesis and physicochemical and catalytic properties of apatite-type lanthanum silicates. Kinetics and Catalysis, 2014, 55, 361-371.	1.0	4
139	Effect of SiO2 on the physicochemical and catalytic properties of VMoTeNbĐž catalyst in oxidative conversion of ethane. Russian Journal of Applied Chemistry, 2016, 89, 1279-1285.	0.5	4
140	Towards the optimization of carbon nanotube properties via in situ and ex situ studies of the growth mechanism. Journal of Structural Chemistry, 2016, 57, 1436-1443.	1.0	4
141	Thermal decomposition of solid solutions in systems of Fe(II), Co(II), and Ni(II) hydrogen maleates with the formation of bimetallic nanoparticles. Russian Journal of Physical Chemistry A, 2017, 91, 136-140.	0.6	4
142	Specific structural features of LnZrOx (Ln: La, Sm) mixed oxides prepared by different methods. Progress in Natural Science: Materials International, 2018, 28, 437-446.	4.4	4
143	Using Current-Voltage Characteristics to Control the Structure of Contacts in Polyethylene Based Composites Modified by Multiwalled Carbon Nanotubes. Journal of Structural Chemistry, 2020, 61, 628-639.	1.0	4
144	Catalytic Behavior of Iron-Containing Cubic Spinel in the Hydrolysis and Hydrothermolysis of Ammonia Borane. Materials, 2021, 14, 5422.	2.9	4

#	Article	IF	CITATIONS
145	Nanoscale Structural Features of Ultra-fine Zirconia Powders Obtained Via Precipitation-hydrothermal Treatment Route. Materials Research Society Symposia Proceedings, 2005, 878, 1.	0.1	3
146	Real Structure - Oxygen Mobility Relationship in Nanocrystalline Doped Ceria-Zirconia Fluorite-Like Solid Solutions Promoted by Pt. Materials Research Society Symposia Proceedings, 2008, 1122, 3.	0.1	3
147	CNT/PMMA Electromagnetic Coating: Effect of Carbon Nanotube Diameter. Fullerenes Nanotubes and Carbon Nanostructures, 2012, 20, 527-530.	2.1	3
148	Structural features of promoted MoVTeNbO catalysts for the oxidative dehydrogenation of ethane. Kinetics and Catalysis, 2015, 56, 788-795.	1.0	3
149	In situ powder X-ray diffraction study of the process of NiMoO4–SiO2 reduction with hydrogen. Journal of Structural Chemistry, 2016, 57, 955-961.	1.0	3
150	Features of the Thermolysis of Fe(II), Co(II), Ni(II), and Cu(II) Salts of Maleic and Phthalic Acids with the Formation of Metal Nanoparticles. Russian Journal of Physical Chemistry A, 2019, 93, 1327-1332.	0.6	3
151	In situ Study of Structural Transformations of the Active Phase of VMoNbTeO Catalysts under Reduction Conditions. Journal of Structural Chemistry, 2019, 60, 1599-1611.	1.0	3
152	Effect of the Conditions of Solution Combustion Synthesis on the Properties of Monolithic Pt–MnOx Catalysts for Deep Oxidation of Hydrocarbons. Kinetics and Catalysis, 2020, 61, 809-823.	1.0	3
153	Electrophysical Properties of Composites Based on Polyethylene Modified with Multi-Walled Carbon Nanotubes with High Content of Fe–Co-Catalyst. Russian Journal of Applied Chemistry, 2020, 93, 586-594.	0.5	3
154	New Solvent-Free Melting-Assisted Preparation of Energetic Compound of Nickel with Imidazole for Combustion Synthesis of Ni-Based Materials. Nanomaterials, 2021, 11, 3332.	4.1	3
155	Graphitization of alumina as a way to stabilize its textural characteristics under hydrothermal conditions. Microporous and Mesoporous Materials, 2022, 341, 112038.	4.4	3
156	Design of Anodes for IT SOFC: Effect of Complex Oxide Promoters and Pd on Activity and Stability in Methane Steam Reforming of Ni/YSZ (ScSZ) Cermets. Materials Research Society Symposia Proceedings, 2006, 972, 1.	0.1	2
157	INFLUENCE OF CURVATURE OF GRAPHENE LAYERS OF MULTI-WALLED CARBON NANOTUBES ON ELECTRICAL PROPERTIES. International Journal of Nanoscience, 2009, 08, 1-4.	0.7	2
158	Advanced Sintering Techniques in Design of Planar IT SOFC and Supported Oxygen Separation Membranes. , 0, , .		2
159	Change in sizes of carbon aggregates and primary particles of the onion-like carbon synthesized by high-temperature annealing of nanodiamond. Russian Chemical Bulletin, 2014, 63, 599-604.	1.5	2
160	Preparation of a copper-polymer composite through the thermolysis of copper(II) succinate. Inorganic Materials, 2014, 50, 945-950.	0.8	2
161	Oxidative dehydrogenation of ethane on VMoTeNbО/Al–Si–O catalysts: Effect of the support on the physicochemical and catalytic properties. Russian Journal of Applied Chemistry, 2017, 90, 1136-1142.	0.5	2
162	Temperature Hysteresis in the Reaction of Methane Oxidation on a Palladium-Doped Manganese Hexaaluminate Catalyst. Kinetics and Catalysis, 2018, 59, 70-82.	1.0	2

#	Article	IF	CITATIONS
163	Synthesis of Highly Dispersed 2D Aluminum Cobalt Oxyhydroxide Compounds Based on Microwave-Activation Products of Crystalline Gibbsite. Inorganic Materials, 2019, 55, 380-389.	0.8	2
164	Quantum Size Effect in Bimetallic Nanoparticles Obtained via Thermolysis of Solid Solutions of Co(II), Ni(II), Zn(II) Salts of Maleic Acid. Russian Journal of Physical Chemistry A, 2020, 94, 2108-2114.	0.6	2
165	The morphology evolution of polyethylene produced in the presence of a <scp>Zieglerâ€type</scp> catalyst anchored on the surface of <scp>multiâ€walled</scp> carbon nanotubes. Journal of Applied Polymer Science, 2021, 138, 50528.	2.6	2
166	Steam Reforming of Methane on Ru and Pt Promoted Nanocomposites for SOFC Anodes. Materials Research Society Symposia Proceedings, 2009, 1217, 1.	0.1	1
167	On the problem of reactor graphite lifetime. Journal of Surface Investigation, 2010, 4, 442-451.	0.5	1
168	A small-angle x-ray scattering study of the nanostructural features of high-ash carbon materials. Journal of Structural Chemistry, 2014, 55, 750-756.	1.0	1
169	Sm-doped praseodymium nickelates-cobaltites and their nanocomposites with Y-doped ceria as promising cathode materials. Integrated Ferroelectrics, 2016, 173, 71-81.	0.7	1
170	Sol–gel synthesis of 2D and 3D nanostructured YSZ:Yb3+ ceramics. Inorganic Materials, 2017, 53, 540-547.	0.8	1
171	Synthesis, physicochemical and catalytic properties of Ni/PrCeZrO catalysts for water-gas shift reaction. Catalysis for Sustainable Energy, 2017, 4, .	0.7	1
172	Production of nano-dimensional crystalline silicon on fast cyclic compression setup. Journal of Physics: Conference Series, 2018, 1105, 012136.	0.4	1
173	Nanocomposite films with UV-Protective Properties Based on Polyethylene with Ultra-Disperse Silicon. International Polymer Science and Technology, 2011, 38, 53-59.	0.1	1
174	Solvent-Free Method for Nanoparticles Synthesis by Solid-State Combustion Using Tetra(Imidazole)Copper(II) Nitrate. Inorganics, 2022, 10, 15.	2.7	1
175	Mechanochemical synthesis of modified hydroxyapatite as a material for implant coating. , 2012, , .		0
176	Production of nanoscale crystalline materials (Si, SiC) by a highly efficient hyperbaric method. Journal of Physics: Conference Series, 2018, 1128, 012100.	0.4	0
177	The method of producing of nano-dimensional silicon carbide by compressing in a cyclic chemical reactor. Journal of Physics: Conference Series, 2018, 1115, 042043.	0.4	0
178	Morphological, Structural, and Catalytic Properties of Pd–CeO2/Al2O3 Compositions and Thereof Coatings in the Oxidation of Methane. Catalysis in Industry, 2019, 11, 323-334.	0.7	0
179	Oxidative Dehydrogenation of Ethane on VMoTeNbĐž/SiO2 Catalysts and the Effect of the Initial Support Compound on Their Physicochemical and Catalytic Properties. Catalysis in Industry, 2020, 12, 226-234.	0.7	0
180	Structural Features and Transport Properties of La(Sr)Fe1-xNixO3-δ〓 Ce0.9Gd0.1O2-δNanocomposites – Advanced Materials for it SOFC Cathodes. , 2010, , .		0

#	Article	IF	CITATIONS
181	Comparative Analysis of Physicochemical Properties of Rutile TiO2 with Hierarchical 3D Architecture Prepared by Liquid Hydrolysis of TiCl4 and Hydrothermal Method. Eurasian Chemico-Technological Journal, 2020, 22, 165.	0.6	0